Acta Chemica Scandinavica, 1993: 47: 358–367
Printed in Belgium – all rights reserved

Copyright © Acta Chemica Scandinavica 1993
ACTA
CHEMICA SCANDINAVICA
ISSN 0904–213X

Scale Formation in Reservoir and Production Equipment during Oil Recovery IV. Experimental Study of $BaSO_4$ and $SrSO_4$ Scaling in Steel Tubings

Mette Rollheim,[a,†] Ramin G. Shamsili,[a] Terje Østvold[a,*] and Anastassios Siamos[b]

[a] Institute of Inorganic Chemistry, NTH, University of Trondheim, N-7034 Trondheim, Norway and [b] Production Technology, Norsk Hydro a.s., N-5020 Bergen, Norway

Rollheim, M., Shamsili, R. G., Østvold, T. and Siamos, A., 1993. Scale Formation in Reservoir and Production Equipment During Oil Recovery IV. Experimental Study of $BaSO_4$ and $SrSO_4$ Scaling in Steel Tubings. – Acta Chem. Scand. 47: 358–367.

Precipitation experiments with $BaSO_4$ and $SrSO_4$ in steel tubings were performed in order to obtain knowledge about the scaling mechanisms for these minerals. Two waters, one containing Ba^{2+} (or Sr^{2+}) the other SO_4^{2-}, were mixed at the entrance of the tubing, and the amount of scale formed in the tubing and the concentration of barium (or strontium) ions in the water flowing in the pipe were measured. The temperature was 40°C, the flow rates 4–6 dm^3/min, inner tube diameters 8–20 mm, duration of each experiments $\leq$4 h. Equimolar solutions of the two minerals were used, and the initial cation concentrations were approximately 30 (Ba^{2+}) and 10 (Sr^{2+}) times the equilibrium concentration.

The presence of an initial thin layer of $BaSO_4$ ($SrSO_4$) on the inside tubing wall resulted in the growth of scale from the very beginning of the experiment. About 95% of the precipitated $BaSO_4$ was deposited as scale when prescaled tubings were used, while only around 75% was found as deposit when initially clean steel tubings were used. Only about 65% of the precipitated $SrSO_4$ was deposited as scale under similar conditions with prescaled 9 and 11 mm tubings.

A comparison between experimental data and model calculations shows that the model is capable of predicting Ba^{2+} and Sr^{2+} concentration profiles in the water phase. The amounts of $BaSO_4$(s) and $SrSO_4$(s) predicted at the different locations in the tube are underestimated. This underprediction is due to nucleation and particle transport processes which are not accounted for in the model.

A linear relationship is indicated between the surface area for crystal growth and the inverse tube radius. The surface areas per unit volume, s, for $BaSO_4$ and $SrSO_4$ precipitation are $s_{BaSO_4} = 18/r$ and $s_{SrSO_4} = 21/r$.

In a previous paper[1] we have discussed the kinetics of scale formation in connection with oil recovery. The development of a scale prediction model that accounts for the kinetics of precipitation for the scaling minerals $CaCO_3$, $BaSO_4$, $SrSO_4$, $CaSO_4$ (anhydrite) and $CaSO_4 \cdot 2H_2O$ (gypsum) was presented. Model calculations performed on a well in the North Sea where $BaSO_4$ scale was formed compared reasonably well with the measured scale thickness along the 2800 m long tubing.[1]

In order to test the model further, experimental work on precipitation of $BaSO_4$ and $SrSO_4$ from a supersaturated flowing aqueous solution on the inside of 20 m long tubing has been performed. Results are presented and discussed in the present paper.

Principles

The kinetics of precipitation of barium and strontium sulfate may be given as eqn. (1), where M refers to barium

$$\frac{d[MSO_4]}{dt} = ks\left(([M^{2+}][SO_4^{2-}])^{1/2} - \frac{K_{sp}^{\circ\,1/2}}{\gamma_{\pm}}\right)^2 \qquad (1)$$

or strontium,[1] the square brackets refer to concentrations in mol per kg H_2O, k is the rate constant for precipitation, s is the specific surface are per volume of solution, K_{sp}° is the thermodynamic solubility product and $\gamma_{\pm}$ is the mean activity coefficient of MSO_4 (aq).

An equation similar to eqn. (1) has been found to describe the rate of barium and strontium sulfate precipitation[2–11] in several seeded growth experiments. The rate is proposed to be controlled by a surface reaction and was therefore independent of stirring rates.

* To whom correspondence should be addressed.
† Present address: Aker Engineering, Tjuvholmen, 0250 Oslo, Norway.

Eqn. (1) reduces to an equation like eqn. (2) when $[M^{2+}]=[SO_4^{2}]$, where $[M^{2+}]$ and $[M^{2+}]^{\circ}$ represent

$$-\frac{d[M^{2+}]}{dt}=ks([M^{2+}]-[M^{2+}]^{\circ})^2 \quad (2)$$

the M^{2+} concentration at time t and at equilibrium, respectively.

Integration of eqn. (2) and using $[M^{2+}]=[M^{2+}]_{init}$ when $t=0$ yields eqn. (3). By increasing the amount of

$$\frac{1}{([M^{2+}]-[M^{2+}]^{\circ})}-\frac{1}{([M^{2+}]_{init}-[M^{2+}]^{\circ})}=kst \quad (3)$$

seed crystals added or decreasing the supersaturation, it was found[2] that the duration and extent of the initial rapid precipitation which could not be described by eqn. (3) was reduced. It was also indicated that for a given supersaturation, a sufficient number of growth sites must be provided initially to obtain a second-order growth rate, otherwise new growth sites were generated by nucleation.

The model

The above second-order rate equations for barium and strontium sulfate precipitation [eqns. (1) and (2)] have been used to calculate scale formation of these salts in a scale prediction computer model developed previously in our laboratory.[1,12–15]

It is observed that the rate of precipitation of one salt may be influenced by precipitation of another substance.[8,10] Such effects are not investigated to such an extent that they can be described by a mathematical model. In the present model calculations each salt has a rate of precipitation as if it was alone.

In the above equations s is a function of the number of active sites for crystallization. If the precipitating mineral is present as scale on an inner tubing wall, these crystals will act as active sites for crystallization of a supersaturated solution of that mineral contained in the tubing. It is our assumption that for moderate supersaturations s is proportional to the surface area of a given length of the inner tubing wall divided by the volume contained in this tube segment.[1] We have suggested that this surface area may be described by eqn. (4). In this equation f is a

$$s=f\frac{A}{V}+C=f\frac{2}{r}+C \quad (4)$$

proportionality factor indicating that the real surface for crystal growth may be much larger than given by the surface area of the tubing, r is the inner tube radius, A is the surface area of the tubing for a given tube length, V is the volume of the same tube section, and C is a constant which may be related to the number of active growth sites in the bulk of the solution.

Eqns. (1)–(4) give the reaction rate of precipitation for the precipitating mineral as long as this reaction is surface-controlled. In tubing this mineral may, as discussed above, grow directly on active sites on the tubing wall or on particles in the bulk of the solution. The number of active sites for crystallization in the bulk phase is given by the number of seed crystals present in the solution. The number and the size of the seed crystals in the aqueous phase will vary along the tubing. This is due to transport of particles from the bulk phase to the pipe wall, a varying influence of precipitation and nucleation mechanisms, and to the removal of adherent mineral from the tubing wall by the flowing fluid. If the growing crystals in the solution settle on the wall of the tubing relatively close to the mixing point, however, the value of C in eqn. (4) should be small for the major part of the tubing.

It is the aim of the present experimental work to test how well eqns. (1)–(4) describe the precipitation of minerals from a flowing supersaturated solution of these minerals. There is a weakness in the experimental technique, however, since we are not able to distinguish between crystals growing directly on the tubing surface and those settling from the solution.

The influence of the oil/water ratio and the wetting properties of the liquid phases in an oil-producing situation is not accounted for. This is of course important to consider if the present model should be used to estimate scaling in an oil producing system. The concentration of foreign particles which could act as crystallization centers would also change the precipitation kinetics considerably. In the present experimental system we have used filtered water to remove such particles.

Experimental

Two waters, one containing $BaCl_2 \cdot 2H_2O$ ($SrCl_2 \cdot 6H_2O$) and the other Na_2SO_4, were mixed at the entrance of the steel tubing. A supersaturated solution was created and precipitation of barite or celestite occured as the aqueous solution flowed through the pipe towards the exit. Precipitation was made either on clean steel tubing, on clean plastic tubing or on tubing covered with barium sulfate or strontium sulfate crystals from a previous run. The apparatus and the procedures are described below.

Apparatus. The three basic sections of the apparatus are the heating system, the mixing and feeding units and the tube section. Fig. 1 shows a schematic drawing of the experimental set-up. Before entering the heater, pure water containing <1 ppm of ionic components passed through four filters of size 10 μm to remove particles in tap water. This is important, since crystallization on foreign particles in the water phase would enhance precipitation on these particles related to precipitation on the tubing wall. Inside the heater, the maximum temperature was 120°C. The hot fluid from the heater was then mixed with a certain amount of cold water, determined by adjusting a thermostat valve, in order for the main water flow to obtain the desired temperature. Before

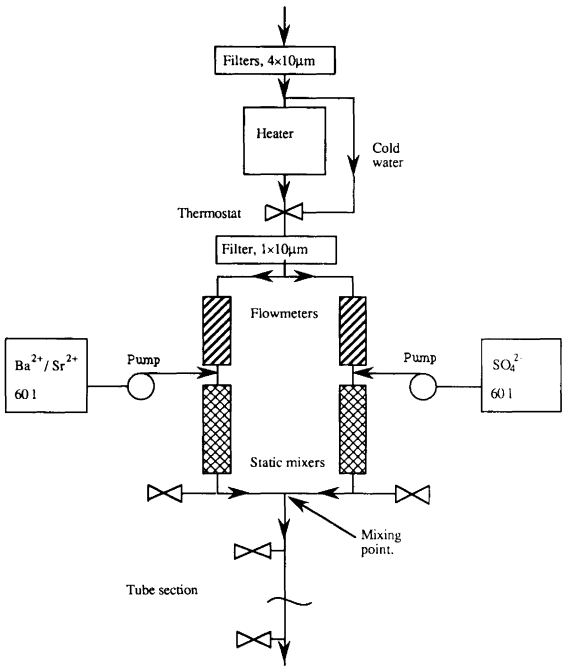

Fig. 1. Schematic drawing of the experimental setup. ⋈ indicate positions where samples could be taken.

entering the mixing unit, the water again passed through a 10 μm filter. Once at the correct temperature, the water was divided into two streams. The flow rates of pure water in these two streams were controlled by adjustable valves and measured with two flow meters. $BaCl_2$ ($SrCl_2$) and Na_2SO_4 solutions contained in two 60 l containers were fed to the water by two manually controlled, variable-speed pumps (Watson-Marlow 503 S/R). The Ba^{2+} and SO_4^{2-} concentrations at the mixing point were approximately 4×10^{-4} M ($[Ba^{2+}] \approx 58$ mg/l), and the Sr^{2+} and SO_4^{2-} concentrations varied between 4.5×10^{-3} and 6.4×10^{-3} M. Both streams entered static mixers shortly after addition of the salt solutions. These mixers were made from a plastic material; their only purpose was to mix properly the concentrated salt solutions with the pure water. Finally, the two streams met in a T-junction at the entrance of the test-tube section which consisted of several steel tubes of 1 m length with an i.d. varying from 8 to 20 mm. Section no. 0 was always of length 0.06–0.14 m. The sections were put together using steel connectors, each with a length of ca. 0.04 m. For practical reasons two of the tube sections, often nos. 7 and 13, formed two bends (180°) to allow the accomodation of the 16 m long tube in the laboratory. As different dimensions of the pipe were used for different experiments, the steel connectors were also of different sizes. However, they always had the same inner diameter as the tubing itself, to prevent as much as possible the formation of eddies in the liquid flow and thereby any enhancement of scaling close to these eddies. A valve was located on each connector in order to make it possible to withdraw samples of the solution at each section during an experiment. Two valves were also located on each main stream just before the mixing point to control the M^{2+} and SO_4^{2-} concentrations before mixing the two solutions.

Chemicals. The chemicals used in the experiments are listed in Table 1.

Experimental procedure. Steel tubing was first cut into sections of length 1 m, and both ends of each section were polished in order to remove sharp edges. After cleaning with strong detergents in order to remove fat and oil and rinsing with pure water, the tubes were dried at 105°C for 2 h. They were then numbered and weighed before being connected. The feed solutions containing Ba^{2+} (Sr^{2+}) and SO_4^{2-} were prepared in two 60 l plastic containers from $BaCl_2 \cdot 2H_2O$ ($SrCl_2 \cdot 6H_2O$) and Na_2SO_4, respectively. The water in which these salts were dissolved was filtered in 10 μm filters. When the desired temperature was obtained in the water flowing through the tube and the liquid flow rate was stable, the pumps were started to feed the salt solutions into the two pure water streams. When the temperature of the aqueous phase was within a given value ± 1°C, the salt solution feed within ± 0.01 l min^{-1} and the flow rates of the two aqueous streams were constant and within ± 0.07 l min^{-1} the experiment could be started. At certain time intervals the outlet temperature, possible leakages, the stability of the fluid flow rate, possible air bubbles in the flowmeters and the stability of the Ba^{2+}/Sr^{2+}, SO_4^{2-} feed were checked. During each experiment solution samples were withdrawn at various locations along the tubing. The sampling was performed by first filling a measured volume of ca. 50 ml of the scale inhibitor solution given in Table 1 into flasks of size 100 ml. The test sample, approximately 50 ml, was then tapped directly into the inhibitor solution. The purpose of the scale inhibitor was to stop any further reaction after sampling of the solution, and a 50 ppm solution was sufficient to stop further precipitation. S491 consists of 37.5 wt.% active substance and its density is 1.207 g cm^{-3}. At the end of an experiment the test tubes were disconnected, rinsed with pure water and dried at 105°C for a minimum of 8 h. The amount of deposit formed on the inner tubing walls was determined as the weight difference of the tube section and the corresponding connector before and after an experiment. Testing of the drying method by pulverizing selected samples and repeating the drying at 105°C was done to ensure that all

Table 1. Chemicals.

Compound	Quality	Manufacturer
$BaCl_2 \cdot 2H_2O$	p.a.	E. Merck, Germany
$SrCl_2 \cdot 6H_2O$	p.a.	E. Merck, Germany
Na_2SO_4	p.a.	E. Merck, Germany
S491, scale inhibitor		Akzo Chemie, Great Britain
Steel tube: <0.17% C, <0.35% Si, <0.40% Mn, <0.05% P, <0.05% S		

the water had left the salt. No difference was observed between the first and this second stage in the drying procedure.

Analytical procedures. The solution samples withdrawn from the test tubing were analyzed by SINTEF (Stiftelsen for Industriell og Teknisk Forskning), Trondheim, Norway, using a Varian 400 AAS atomic absorption spectroscopy unit. Precision of the atomic adsorption analysis is ± 0.1 mg l^{-1}.

Results and discussion

Experimental uncertainties. The measured concentrations of Ba^{2+} and Sr^{2+}, and in some cases also the SO_4^{2-} concentrations, in the aqueous phase along the steel tubing show some scatter. To present this concentration variation in a consistent form the relative standard deviation is calculated using eqn. (5). In this equation SD is the

$$\mathrm{SD}(\%) = \left(\sum_{i=1}^{n} (y_i - \bar{y})^2/(n-1) \right)^{1/2} 100/\bar{y} \qquad (5)$$

relative standard deviation, y_i is the measured concentration, $\bar{y}$ is the average concentration at each sampling point and n represents the number of samples taken at each location. The average relative standard deviation, $\overline{\mathrm{SD}}$, for an experiment, was also calculated, and is given by eqn. (6), where N is the number of positions at which

$$\overline{\mathrm{SD}} = \sum_{i=1}^{N} \mathrm{SD}(\%)_i/N \qquad (6)$$

samples were taken.

$\overline{\mathrm{SD}}$ values for the Ba^{2+} profiles are around 2–3 %. This variation is larger than expected from the atomic absorption spectroscopy analysis. The reason for this scatter may be the practical difficulty of sampling a solution undergoing a chemical reaction. The relative standard deviation shows no variation along the tubing. This indicates proper mixing at the tubing entrance. Similar observations were made for the Sr^{2+} concentrations.

The iron content of the solution was found to increase slightly with increasing tube length. This is due to corrosion of the steel tube. However, the concentration was less than 0.5 mg l^{-1} at the tube exit, and its influence on the precipitation rate is probably insignificant.

Weighing of the mineral deposit was performed using a balance with a precision of ± 0.01 g.

The temperature at the tube exit was measured during each experiment at intervals of about 30 min, and its variation was ± 1°C. The difference in temperature between the mixing point and the tube exit was ca. 1°C. The temperature difference between the inside and the outside of the tubing wall was measured to be less than 0.5°C. The abovementioned temperature variations are so small that an influence on rate constants and solubility products can be neglected.

The largest pressure drop due to friction in the present experimental series was estimated to be ca. 0.7 atm. Since $\mathrm{d}\ln K_{sp}/\mathrm{d}P = 0.002$ atm^{-1} at 1 atm, the change in solubility of $BaSO_4$ due to this pressure drop can be neglected.[14] The same was true for the $SrSO_4$ experiments.

Close to the steel tubing, the barium and strontium sulfate scale was slightly brownish owing to corrosion products of iron oxide. This was especially true for the preliminary experiments for which the duration of the test was 8 or 12 h. When care was taken to clean the tubing properly, to reduce the duration of the experiments to 4 h or less and to start the drying procedure as soon as possible after shut-down of the experiment, the corrosion problem was reduced considerably. Only a small fraction ($\ll 1$ wt. %) of the weight increase observed could be due to corrosion products.

During scaling there is a small change in the inner tube diameter. This effect is especially important for tubes with the smallest diameter (9 mm). In the beginning of the tube the supersaturation is large and the scaling rate high. The inner diameter is therefore reduced faster at the beginning than at the end of the pipe. During prescaling of the pipe, the prescaling period was divided into two intervals. In the second period the tubing was connected in the opposite direction. The time intervals were adjusted in such a way that an even layer of scale throughout the pipe was obtained.

Scale profiles. The reproducibility of the scale profiles may be estimated by calculating the difference in scale obtained at each location between two runs, and from these values calculating an average SD for the experiment. For $BaSO_4$ this SD was found to be 0.32 and 0.14 g m^{-1} for initially clean (i.d. = 15 mm) and initially prescaled (i.d. = 8 mm) tubings, respectively. The reproducibility seems to be better for prescaled tubings. This is due to a uniform crystal growth process on the prescaled surface.

For some of the $SrSO_4$ experiments we had some problems with the Sr^{2+} and SO_4^{2-} feeding pumps which introduced a slow variation with time in the concentration of these ions at the mixing point. Only successful experiments are reported. The reproducibility of two scale profiles estimated as described above for a prescaled 11 mm i.d. tubing was not as good as for $BaSO_4$ giving an SD of 1 g m^{-1}. This is, however, partly due to the larger amount of scale formed in the $SrSO_4$ case.

When comparing different experiments where the total amount of Ba^{2+} introduced was the same, the lowest liquid flow rates gave the highest amount of scale. This is due to a higher residence time at smaller flow rates. A comparison of experiments also showed that a decreasing tube diameter gave increasing amounts of scale. The main reason is the increased surface area available for growth per volume of solution for reduced tube diameters.

Substitution of some of the 1 m initially clean steel tube sections with plastic (polyvinyldifluoride) tube sections showed that it was more difficult for an initial crystal

layer to form on the plastic surface. Once the first crystal layer had formed, however, the tubing material had no influence on the growth rate as expected.

Variations in temperature ($25 \leqslant T/°C \leqslant 55$) did not give rise to any unexpected effects. More MSO_4 was observed at higher temperatures mainly in the beginning of the tube, in agreement with higher reaction rates at higher temperatures. Typical results are shown in Fig. 2 for $BaSO_4$. Experiments performed with initially clean steel tubings gave less scale then with prescaled tubings. This is mainly due to an earlier start of the growth process on the tubing wall when the tubings are covered with sulphate crystals. Another less important reason for the larger amount of scale formed in the prescaled tubings is an easier particle deposition process on the rougher scale surface.

M^{2+} concentration profiles. The M^{2+} concentration in the liquid at a given tube location decreased with time when initially clean tubings were used. This is due to a lower precipitation and growth rate of MSO_4 when few MSO_4 crystals are available for crystal growth. The supersaturation of the aqueous phase is therefore kept at a higher level. The increasing amount of scale on the tube wall increases the growth rate until the tube is covered with scale. Once a smooth layer of scale has been formed, a further reduction in the supersaturation at a given position does not occur. In Fig. 3 Ba^{2+} concentrations are shown as a function of location and time for an experiment where the tube was prescaled with $BaSO_4$. The samples were withdrawn at about 0.7 h (open symbols) and at about 3.1 h (filled symbols) after start. The period with changing Ba^{2+} concentrations at a given location is almost eliminated. A small reduction in concentration may occur with time, however, due to a reduction in the inner tube diameter caused by the build-up of scale.

In Figs. 2–4 a reduction in $[Ba^{2+}]$ with tube length is observed as expected. In Fig. 4 $[Ba^{2+}] = 56\ mg\ l^{-1}$ at the tube entrance and $[Ba^{2+}] \approx 49\ mg\ l^{-1}$ at 0.14 m. This is a larger reduction in concentration per metre of tubing than expected from the concentration reduction observed

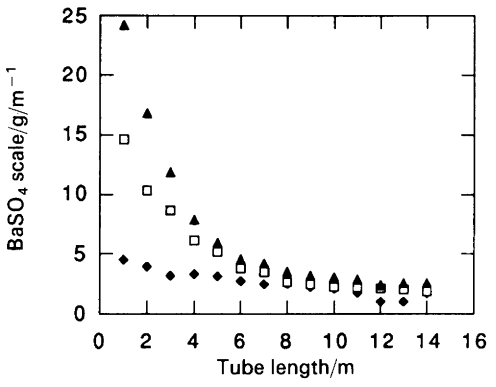

Fig. 2. $BaSO_4$ scaling in a 9 mm i.d. tubing as function of distance from the mixing point and temperature, flow rate: 3.77 l min^{-1} (◆) 25, (□) 40, (▲) 55°C.

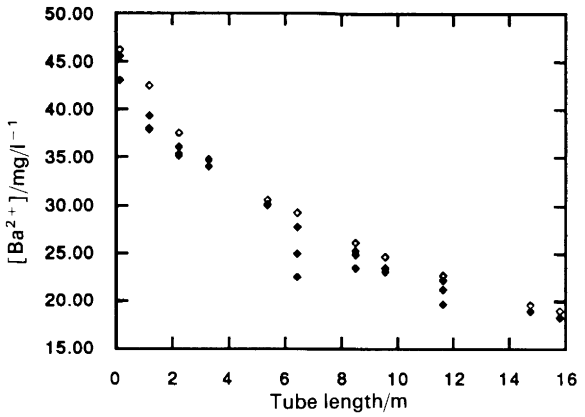

Fig. 3. Ba^{2+} concentrations in the aqueous phase along initially prescaled steel tubing as a function of location and sampling time. Temperature, 40°C; flow rate, 4 l min^{-1}; duration, 4.0 h; i.d. diameter, 14 mm; saturation concentration, $[Ba^{2+}]° \approx 2\ mg\ l^{-1}$ (calculated using equilibrium model). (◇) 0.7 h; (◆) 3.1 h, $\overline{SD}$, 2.95% [eqns. (5) and (6)].

later in the tubing, and must be due to nucleation in addition to crystal growth in the volume where the two liquids meet. The supersaturation is at its maximum in this region and gives rise to a higher degree of nucleation than later in the tubing where MSO_4 crystals are available in a sufficient amount to reduce the nucleation relative to the growth process.[2]

The rate equation, eqn. (1), describes the concentration decrease along the tubing, or the rate of formation of $BaSO_4$(s) as long as nucleation is insignificant. The *s*-term in this equation is a function of the number of active sites for crystallization. In order to model crystal growth and scale formation a model for *s* is needed. Eqn. (4) relates *s* to the surface area divided by volume of a tube segment. In order to test this equation, the measured concentration

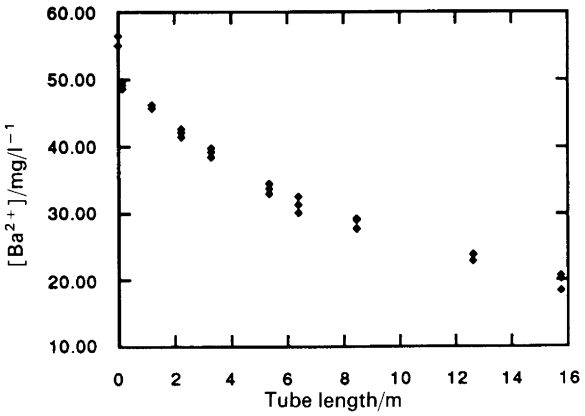

Fig. 4. Ba^{2+} concentrations in the aqueous phase in initially prescaled steel tubing as a function of location. Temperature, 40°C; flow rate, 6 l min^{-1}; duration, 4.0 h; saturation concentration, $[Ba^{2+}]° \approx 2\ mg\ l^{-1}$ (calculated using equilibrium model);[13–15] inner tube diameter, 12 mm; (◆) sampling time, 3.3 h; $\overline{SD}$, 2.38% [eqns. (5) and (6)].

profile of M^{2+} in the aqueous phase along the tubing was used. Plotting the left-hand side of the integrated rate equation, eqn. (1) or eqn. (3) when $[M^{2+}] = [SO_4^{2-}]$, versus time gives a straight line if the model fits the data. The slope of this straight line represents the ks-term. When the rate constant, k, is known,[1] s may be calculated. The equilibrium value of the M^{2+} concentration was obtained using an equilibrium model developed in our laboratory.[15]

MODFIT,[16] a general computer program for nonlinear parameter estimation, was used to fit data to the integrated rate equation. In Fig. 5 the rate equation in the integrated form is shown. When the left-hand side of eqn. (3) is plotted versus time straight lines are obtained as expected. Straight lines, as seen in Fig. 5, were observed for all experiments with prescaled tubings. At the mixing point nucleation processes will probably occur as discussed previously, meaning that the precipitation kinetics is different than that observed later in the experiment. This means that the straight lines shown in Fig. 5 do not necessarily pass through origo, which represents the mixing point of the two liquids.

s-Values may be obtained for experiments with different tube diameters. In Fig. 6 s-values are plotted as a function of the inverse tube radius. Heavily prescaled 9 and 15 mm tubes were measured to be close to 8 and 14 mm i.d. when the experiments started. For large tube diameters no experimental values are obtained, but measurements of scale build-up in production tubing of a North Sea well were available and tested in a simulation.[1] Model calculations on this well gave a scale build-up profile along the

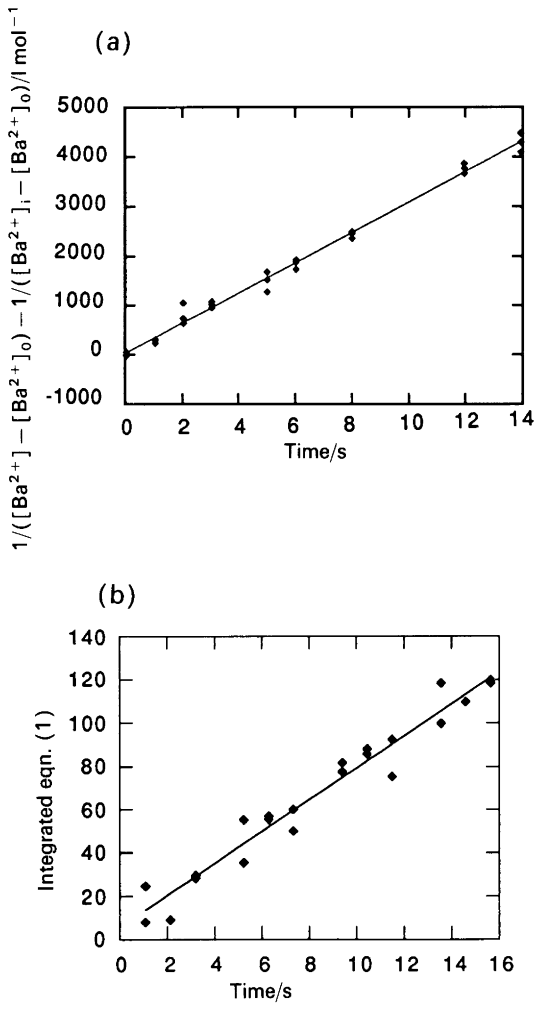

Fig. 5. Integrated rate equation as a function of time. (a) Precipitation of $BaSO_4$ in 9 mm i.d. steel tubing at 40°C. Flow rate, 4 l min^{-1}; duration, 4.0 h; (◆) experimental data, (—) model curve [eqn. (3)]. (b) Precipitation of $SrSO_4$ in 9 mm i.d. steel tubing at 40°C. Flow rate, 1.5 l min^{-1}; duration, 5.6 h; (◆) experimental data; (—) model curve, eqn. (1) was used since $[Sr^{2+}] \neq [SO_4^{2-}]$.

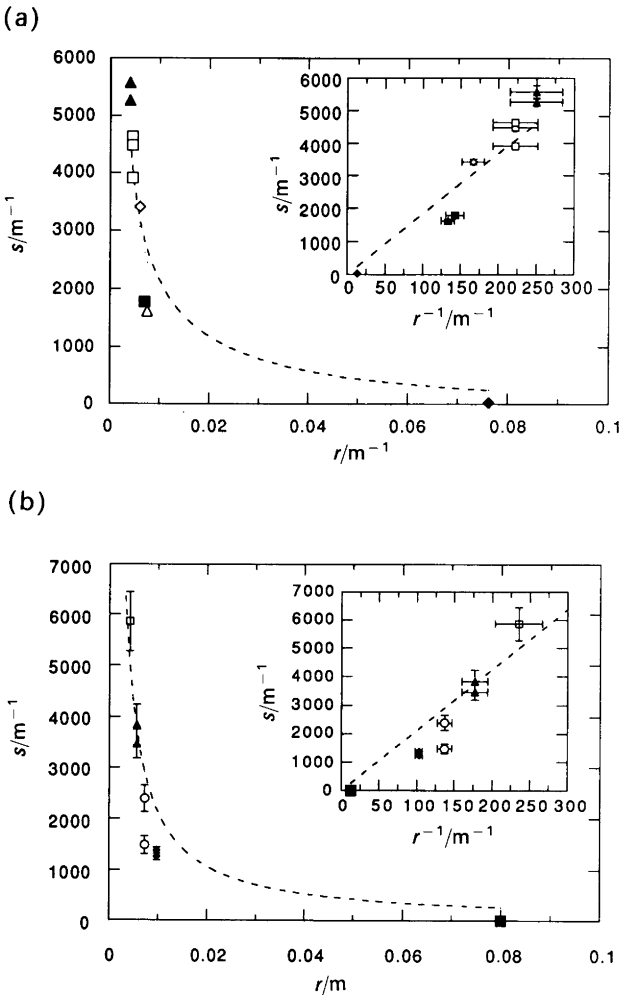

Fig. 6. Specific surface area for crystallization per volume of solution plotted versus inner tube radius. The steel tube radius was slightly reduced because of scale. This is taken into account when making the plot. (a) $BaSO_4$ precipitation in prescaled steel tubing: (▲) 8, (□) 9, (◇) 12, (■) 14, (△) 15 mm i.d.; (◆) $s = A/V$ used in simulation of $BaSO_4$ precipitation in an oil-producing well in the North Sea;[1] (---) model curve, eqn. (4) with $C = 0$. (b) $SrSO_4$ precipitation in prescaled steel tubings: (□) 8, (▲) 11, (○) 14, (◆) 19 mm i.d.; (■) A/V for 16 cm i.d. tubing; (---) model curve, eqn. (4) with $C = 0$.

2800 m long tubing from the bottom to the well head which agreed reasonably well with the scale thickness measured.[1] The s-value used in this simulation was obtained from eqn. (4) with $f_1 = 1$ and $C = 0$. In this well the oil/water weight ratio was 0.425. This means that the value of s used in the simulation might be incorrect, first because the wetting properties of the two liquids on the tubing is not considered in this case, and secondly because the s-term must depend on the volume of the aqueous phase only and not on the total volume of a given tube segment, since only parts of this segment are filled with the supersaturated $BaSO_4$ solution.

The straight lines for the s versus $1/r$ plots shown in Fig. 6 indicate a linear relationship between the specific surface area per volume of solution and the inverse tube radius. It can also be seen from Fig. 6 that the extrapolation of the model eqn. (4) to tube radii in practical use seems to be reasonable. In Fig. 6 a plot is also shown of s versus r to indicate that the experimental region is far from the region of practical tube radii. It is, however, important to note that experimental data indicate that the precipitation processes of both $BaSO_4$ and $SrSO_4$ are surface-controlled.[2-11] This must imply that $s \to 0$ when $r \to \infty$. With this in mind it seems that the present data are reasonable and that the f values for $BaSO_4$, $2f = 18$, and $SrSO_4$, $2f = 21$, precipitation should be useful in a scale prediction model even for larger tube radii than those studied in the present work.

Mineral precipitation versus mineral scaling. The total amount of solid mineral formed during an experiment, according to the cation concentration decrease over the tubing, was calculated using eqn. (7). The results were compared with the amount of scale observed in the tubing. In this equation, w is the weight of $MSO_4(s)$ formed

$$w = ([M^{2+}]_{entrance} - [M^{2+}]_{exit})\, q M_M \tau \qquad (7)$$

during the experiment, $[M^{2+}]_{entrance}$ and $[M^{2+}]_{exit}$ are the M^{2+} concentrations (in mol kg^{-1} H_2O) at the tubing entrance and exit, respectively, q is the fluid flow rate (kg H_2O h^{-1}), M_M is the molar weight of MSO_4 and τ is the duration of the experiment (in h).

Any decrease in the M^{2+} concentration results in $MSO_4(s)$. Since the concentration at a given location was not constant during experiments when clean tubing was used at the start of an experiment, only an estimate of the precipitated amount of MSO_4 could be obtained for such cases. This estimate was obtained in the following way: the $[Ba^{2+}]_{exit}$ obtained 1 h after start was used to calculate the amount of $BaSO_4(s)$ formed during the first hour, the $[Ba^{2+}]_{exit}$ obtained 2 h after start was used to calculate the amount of $BaSO_4(s)$ formed during the second hour, and so on. For experiments with prescaled tubing, the measured $[Ba^{2+}]_{ext}$ was used for the total duration of the experiment, since this concentration is almost constant. In Fig. 7 the total amount of scale measured is compared with the results obtained using

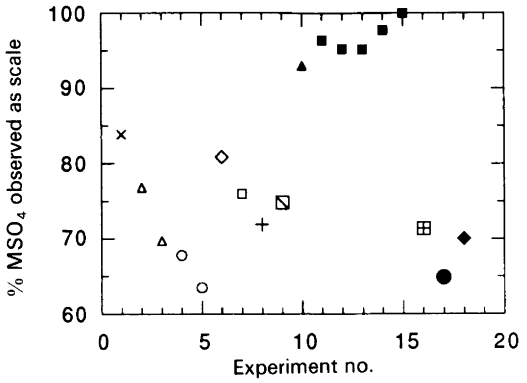

Fig. 7. Scale observed relative to the amount calculated by eqn. (7). Filled symbols represent experiments with initially prescaled tubing. Other symbols represent initially clean steel tubing. Total tube length 16 m. $BaSO_4$: (□, ⊞, ■) 9 mm i.d., flow rate 4 l min^{-1}, 4 h duration; (×) 9 mm i.d., flow rate 6 l min^{-1}, 4 h duration; (△, ▲) 12 mm i.d., flow rate 6 l min^{-1}, 4 h duration; (○) 15 mm i.d., flow rate 6 l min^{-1}, 4 h duration; (▼) 9 mm i.d., flow rate 5 l min^{-1}, 4 h duration; (+) 9 mm i.d., flow rate 6 l min^{-1}, 2.7 h duration; (⊠) 9 mm i.d., flow rate 5 l min^{-1}, 3.2 h duration. $SrSO_4$: (●) 8 mm i.d., flow rate 1.5 l min^{-1}, 5.6 h duration; (◆) 11 mm i.d., flow rate 2.7 l min^{-1}, 3.2 h duration.

eqn. (7). On average more than 95% of the $BaSO_4$ precipitated was observed as scale in experiments where an initial scale layer was present. This indicates that the major precipitation process is governed by a surface-controlled reaction and that eqns. (1)–(4) will describe the scaling process. When experiments were performed with initially clean steel tubing, however, only 65–85% of the available solid $BaSO_4$ was deposited. A significant amount of the precipitate was transported through the tubing.

Comparison between experimental data and model calculations. Simulations were performed using s obtained as described above. A comparison between experimental data and model was made. Examples of simulated Ba^{2+} and Sr^{2+} concentration profiles are shown in Fig. 8. The value of s which is used is that obtained from the experimental data shown in Fig. 6. The kinetic model seems to be able to predict the concentration profile of M^{2+} in the tubing, but the model calculation must start from a location in the tubing where crystal growth is the dominating precipitation process. This means that the model should also be able to predict the amount of $MSO_4(s)$ formed. The growth of scale, however, may not be related directly to the concentration decrease, since crystals will also to some extent form and grow in the solution. In Fig. 9 both the experimental and a simulated scale profile are shown. The data are from the same experiment as shown in Fig. 8. The model predicts less scale than experimentally observed. This is probably due to the nucleation and precipitation of $MSO_4(s)$ in the liquid phase just after the mixing point. Small amounts of MSO_4 were observed at the tube exit. This means that the

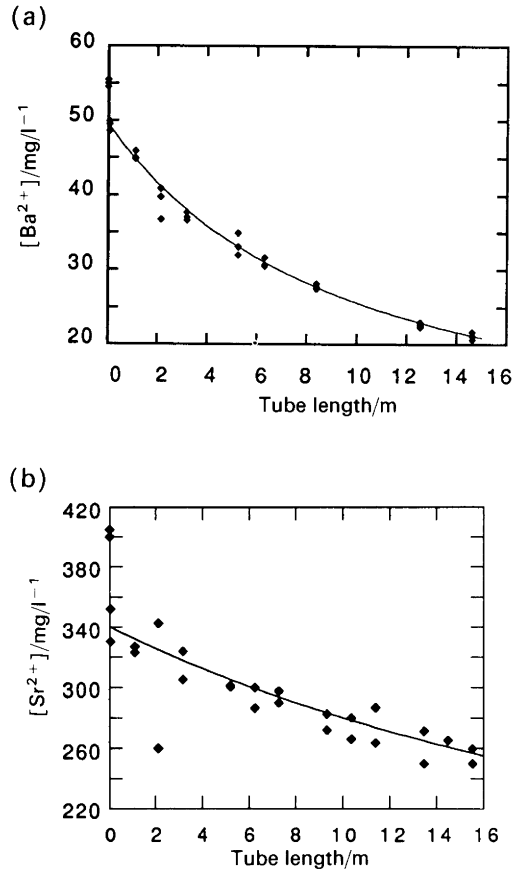

Fig. 8. M^{2+} concentrations in steel tubing covered with MSO_4 crystals during MSO_4 precipitation at 40°C. (a) $BaSO_4$ precipitation: (◆) flow rate 4 l min^{-1}, 9 mm i.d., 4 h duration; (——) model curve, eqn. (3); start of model calculation at 0.06 m, $s = 3910$ m^{-1}. (b) $SrSO_4$ precipitation: (◆) flow rate 3.4 l min^{-1}, 8 mm i.d., 5.6 h duration; (——) model curve, eqn. (3); start of model calculation at 0.052 m, $s = 6270$ m^{-1}.

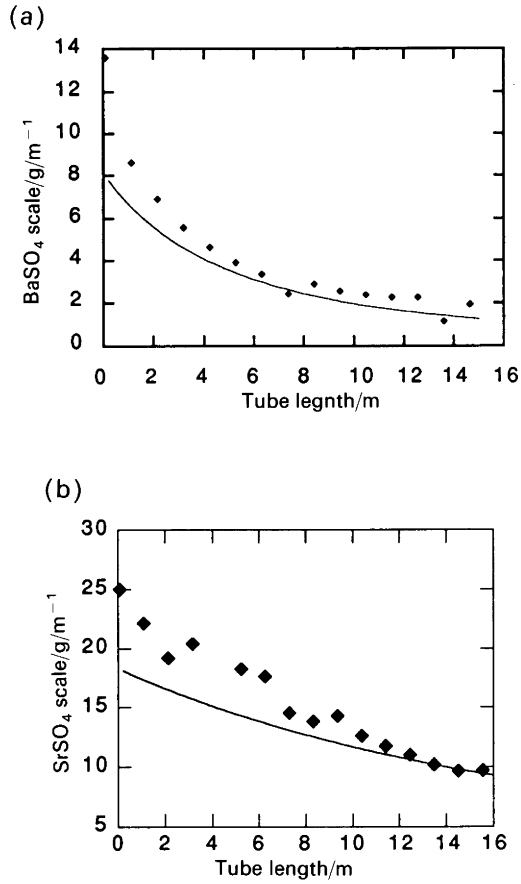

Fig. 9. Scale profile in steel tubing initially prescaled with MSO_4. Temperature 40°C. (a) $BaSO_4$ precipitation: (◆) flow rate 4 l min^{-1}, 9 mm i.d., 4 h duration, $[Ba^{2+}]_{init} = 58$ mg l^{-1}; (——) model curve, eqn. (1); start of calculation at 0.06 m, $s = 3910$ m^{-1}. (b) $SrSO_4$ precipitation: (◆) flow rate 3.4 l min^{-1}, 8 mm i.d., 5.6 h duration, $[Sr^{2+}]_{init} = 400$ mg l^{-1}; (——) model curve, eqn. (1); start of calculation at 0.052 m, $s = 6270$ m^{-1}.

$BaSO_4$ precipitated in the solution will be transported along with the liquid and deposit somewhere in the tube. In the $SrSO_4$ precipitation experiments a considerable amount of $SrSO_4$ was lost through the tube exit. For all the data obtained with prescaled tubings the comparison between measured and calculated scale profiles were similar to those shown in Figs. 8 and 9.

Modelling precipitation in a system of relevance to oil production. In a recent paper we presented a simulation of the scale build-up in 2800 m long production tubing where the watercut was 57.5%. The simulation fitted well with the scale thickness measured when the tubing was pulled up. There are many uncertainties associated with such simulations. In our calculation s was simply set equal to A/V and no correction was made for the 42.5% oil content of the flowing liquid. According to the present data these oversimplifications underestimate the s-value by at least a factor of 10. During oil production the time for nucleation of scale on a clean surface is probably very short compared with the time it takes for the precipitating mineral to grow thick layers of scale. It may therefore be less important in a real system than in the laboratory experiments to consider this nucleation time when the amount of scale is to be calculated from model considerations. It should also be noted that a mixture of oil and water may behave quite differently than a pure aqueous phase. If the surface where the crystals grow is oil wetting, the conditions for scaling are quite different than in the present case. A much lower scaling rate would probably then be observed.

In the previous paper mentioned above[1] a model for simulation of mineral precipitation in a flowing liquid close to an oil production well was presented. The solution, being at equilibrium a few meters from the center of the well, was flowing through the porous medium and into the well. At some distance from the well, equilibrium may be assumed for the slightly soluble minerals, since liquid movements are slow and there is a large surface-to-volume ratio in porous systems. The drastic change in

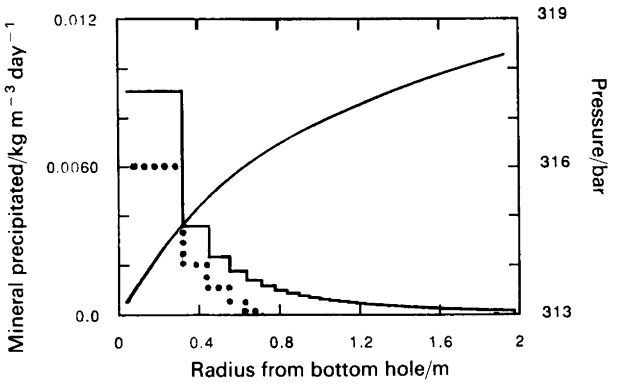

Fig. 10. Precipitation of $BaSO_4$ in the well area as a function of distance from the well centre. The waters were mixed at 2 m from the centre of the tubing and chemical equilibrium was allowed to be established. Oil flow rate = 1792 S m^3 day^{-1}, water cut = 57.5%, T = 90.2°C, porosity of formation 23.6%; (——) equilibrium model; (·····) kinetic model with $s = 3.3 \times 10^5$ m^{-1} $r \simeq 0.1$ mm [eqn. (4)] × 2 due to 50% water cut.

cross-section for liquid flow close to a production well will create a considerable pressure gradient in this area. This pressure gradient will result in supersaturation and mineral precipitation.

Using the present results, the scale prediction models[1,14,15] and a flow model[1] for liquid flow in a porous system, we can estimate the effect of a pressure gradient on mineral precipitation in the well bore area. This is a critical area for liquid transport during oil recovery, since changes in the porous system by movement of fines and mineral precipitation may easily reduce the permeability of the system, with resulting production losses. In Table 2 the sea and formation waters used in the present calculation are given. As can be observed from Table 2, the Ba^{2+}, Sr^{2+} and Ca^{2+} concentrations are small. In many oil fields much higher concentrations may be observed, with a higher potential risk for scaling problems. As an example we have estimated the precipitation occurring if we produced at 90% formation water – 10% sea water mixture (data given in Table 2) from a well with a production rate of 1792 S m^3 day^{-1} of oil and with a watercut of 57.5%. From Fig. 10 it may be seen that $BaSO_4$ is precipitated in the well area in increasing amounts as the pressure is decreasing. The kinetic model gives lower values than the equilibrium model, as expected, but the smaller the pores the larger is the s-value in eqn. (1). It is reasonable to believe that for very small pores there will not be a significant difference between the real precipitation and that calculated by the equilibrium model. The amount precipitated in this way may be sufficient to reduce significantly the permeability of the formation in the near-well area over a period of a few months if injection water and formation water mix close to the well.

Table 2. Sea water and formation water compositions as given by chemical analysis at 1 atm and 20°C.

	Concentration/mg l^{-1}	
Ion	Sea water	Formation water
Na^+	12465	14859
K^+	—	—
Mg^{2+}	1130	335
Ca^{2+}	450	1275
Sr^{2+}	9	335
Ba^{2+}	—	50
Cl^-	20950	26200
SO_4^{2-}	3077	—
HCO_3^-	170	415
pH	8.13	6.20

Conclusions

The present data indicate that precipitation of MSO_4 scale (M = Ba^{2+} and Sr^{2+}) is formed on tubing walls by a process which is mainly determined by a surface controlled reaction. The proposed scale prediction model is able to predict the concentration of the dissolved supersaturated mineral in the flowing liquid. The calculated amount of precipitate formed on the walls of the tubing is, however, underestimated. This is due to nucleation and particle transportation processes which are not accounted for in the present model.

A linear relationship between the number of active sites for crystal growth and the inverse tube radius is observed for small tube radii as predicted for surface-controlled precipitation.

Acknowledgment. The present project was supported financially from STATOIL, Norsk Hydro and The Royal Norwegian Council for Scientific and Industrial Research.

References

1. Granbakken, D. B., Haarberg, T., Rollheim, M., Østvold, T., Read, P. and Schmidt, T. *Acta Chem. Scand. 45* (1991) 892.
2. Nancollas, G. H. and Purdie, N. *Trans. Faraday Soc. 59* (1963) 735.
3. Liu, S. T. and Nancollas, G. H. *J. Colloid Interface Sci. 52* (1975) 582.
4. Nancollas, G. H. and Liu, S. T. *Soc. Petr. Eng. J.* (December 1975) 509.
5. Liu, S. T. Nancollas, G. H. and Gasiecki, E. A. *J. Cryst. Growth. 33* (1976) 11.
6. Leung, W. H. and Nancollas, G. H. *J. Cryst. Growth. 44* (1978) 163.
7. Hostomsky, J., Rathousky, J. and Skrivanek J. *Cryst. Res. Technol. 16* (1981) 759.
8. Gardner, G. L. and Nancollas, G. H. *J. Phys. Chem. 87* (1983) 4699.
9. Sühnel, O. and Handlirova, M. *Industrial Crystallization 84*, Elsevier, Amsterdam 1984, p. 281.
10. Campbell, J. R. and Nancollas, G. H. *J. Phys. Chem. 73* (1969) 1735.
11. Sühnel, O. and Handlirova, M. *Cryst. Res. Technol. 19* (1984) 477.

12. Rollheim, M. *Thesis.* Institute of Inorganic Chemistry The Norwegian Institute of Technology, Trondheim, Norway 1991.
13. Haarberg, T., Seim, I., Skjørholm, S. J., Østvold, T. Read, P. and Schmidt, T. *Proc. Third Int. Symp. Chemicals in the Oil Industry*, Manchester, April 19-20, 1988, Ogden, London 1989, p. 121.
14. Haarberg, T., Seim, I., Granbakken, D. B., Østvold, T., Read, P. and Schmidt, T. *SPE Prod. Eng.* February 1992, 75.
15. Haarberg, T. *Thesis.* Institute of Inorganic Chemistry, The Norwegian Institute of Technology, Trondheim, Norway 1989.
16. Hertzberg, T. Internal report. Institute of Chemical Engineering, The Norwegian Institute of Technology, Trondheim, Norway 1983.

Received August 14, 1992.